

AdaVBoost: Mitigating Hallucinations in LVLMs via Token-Level Adaptive Visual Attention Boosting

Jiacheng Zhang^{*1,2} Feng Liu² Chao Du¹ Tianyu Pang¹
 GitHub: <https://github.com/JiachengZ01/AdaVBoost>

Abstract

Visual attention boosting has emerged as a promising direction for mitigating hallucinations in *Large Vision-Language Models* (LVLMs), where existing methods primarily focus on *where* to boost by applying a predefined scaling to the attention of method-specific visual tokens during autoregressive generation. In this paper, we identify a fundamental trade-off in these methods: a predefined scaling factor can be too weak at some generation steps, leaving hallucinations unresolved, yet too strong at others, leading to new hallucinations. Motivated by this finding, we propose **AdaVBoost**, a token-level visual attention boosting framework that adaptively determines *how much* attention to boost at each generation step. Specifically, we introduce *Visual Grounding Entropy* (VGE) to estimate hallucination risk, which leverages visual grounding as a complementary signal to capture evidence mismatches beyond entropy. Guided by VGE, **AdaVBoost** applies stronger visual attention boosting to high-risk tokens and weaker boosting to low-risk tokens, enabling token-level adaptive intervention at each generation step. Extensive experiments show that **AdaVBoost** significantly outperforms baseline methods across multiple LVLMs and hallucination benchmarks.

1. Introduction

Hallucination is a long-standing challenge in Large Vision-Language Models (LVLMs) (Huang et al., 2023; Liu et al., 2023; Bai et al., 2024). LVLMs often over-rely on language priors, thereby diminishing the role of the visual modality during autoregressive generation (Liu et al., 2024b). As a consequence, LVLMs may generate contents that are inconsistent with the visual input (i.e., hallucinations).

^{*}This work was done during Jiacheng Zhang’s associate membership at Sea AI Lab. ¹Sea AI Lab ²The University of Melbourne. Correspondence to: Tianyu Pang <tianyupang3@gmail.com>.

Preprint. February 17, 2026.

To address this issue, visual attention boosting emerges as a promising direction due to its effectiveness and efficiency in hallucination mitigation (Liu et al., 2024b; Yin et al., 2025; Xie et al., 2025; Zhao et al., 2025). Unlike other hallucination mitigation methods that require additional training (Zhao et al., 2023b; Yue et al., 2024; Xiao et al., 2024; Xing et al., 2024; Sun et al., 2024; Zhao et al., 2024) or multiple forward passes (Huang et al., 2024; Leng et al., 2024; Wang et al., 2024; Huo et al., 2024; Jiang et al., 2024), visual attention boosting methods directly amplify the attention weights of visual tokens during autoregressive generation within a single forward pass, making them *training-free* and *efficient* (Yin et al., 2025; Xie et al., 2025; Zhao et al., 2025). Existing visual attention boosting methods primarily focus on *where* to boost, i.e., selecting which visual tokens to emphasize, and scale their attention weights using a predefined scaling factor across all generation steps.

However, we identify a fundamental trade-off in existing visual attention boosting methods, as illustrated in Figures 1a and 1b. Specifically, applying a uniform visual boost produces a *dual effect*: while a predefined scaling factor successfully resolves many hallucinations, it also introduces new hallucinations that are absent from the original response, which we term *over-boosted* hallucinated tokens (see Figure 1a), indicating that the predefined scaling factor can be overly strong at certain generation steps. Meanwhile, a non-trivial portion of hallucinated tokens present in the original response remain unresolved after uniform boosting (see Figure 1a). Most of these hallucinations are *under-boosted*, in the sense that they can be resolved by further increasing the visual boosting strength (see Figure 1b), suggesting that the same scaling factor can be too weak at other generation steps. More importantly, both under-boosted and over-boosted hallucinated tokens can *co-exist* within the same response across different LVLM architectures (see Figure 2). Taken together, these observations indicate that the reliance on visual attention is inherently uneven across tokens during generation, highlighting the need for token-specific visual interventions for more effective hallucination mitigation. However, it is infeasible to heuristically determine the appropriate amount of attention to boost for each token during generation, motivating us to make a *first at-*

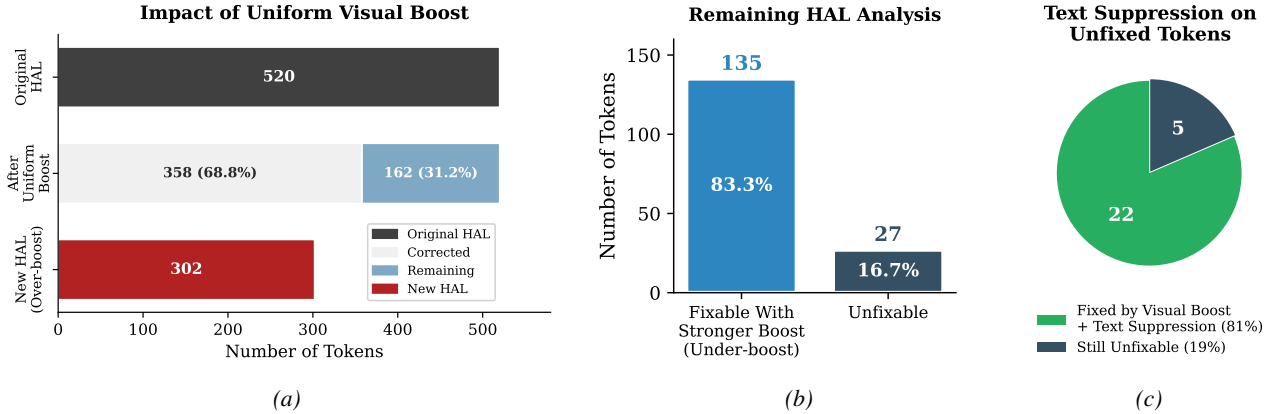


Figure 1. Proof-of-concept experiments. We randomly sample 200 examples from the AMBER benchmark (Wang et al., 2023) and use GPT-5-mini (OpenAI, 2025) as a judge to determine whether a token is hallucinated. The full prompts and detailed justifications are provided in Appendix A. Following the experimental setting of Liu et al. (2024b), we set the scaling factor to 1.2. All experiments are conducted on LLaVA-NeXT-7B (Liu et al., 2024a). (a): Effects of uniform visual attention boosting on hallucinated tokens using a pre-defined scaling factor (i.e., 1.2). Out of 520 hallucinated tokens in the original responses across 200 images, 358 tokens are successfully corrected after boosting visual attention. However, 162 hallucinated tokens remain unresolved, indicating that the predefined scaling factor might be insufficient for some generation steps. Meanwhile, the same scaling factor can be overly aggressive for other tokens, leading to 302 over-boosted hallucinated tokens that are absent from the vanilla response. (b): Analysis of the 162 remaining hallucinated tokens. 135 tokens become non-hallucinatory with stronger visual boost (i.e., larger than 1.2), indicating they are under-boosted at the current scaling factor. Taken together, these observations highlight the need for token-specific visual interventions. (c): Investigation of unfixable tokens. For the remaining 27 tokens that visual boosting alone cannot resolve, we apply attention suppression on text input tokens as a complement to visual boosting. Notably, 22 tokens become non-hallucinatory, leaving only 5 hallucinated tokens.

tempt toward a framework that adaptively determines *how much* attention to boost at each generation step.

To this end, we propose **AdaVBoost**, a training-free, token-level framework that first estimates hallucination risk for each token, and then uses this risk to adaptively boost visual attention during autoregressive generation.

To implement **AdaVBoost**, we need to understand how to quantify hallucination risk at each generation step. There are several well-established techniques to achieve this purpose, such as token probability-based methods (Takayama & Arase, 2019; Malinin & Gales, 2021), output consistency-based methods (Zhao et al., 2023a; Nikitin et al., 2024) and internal state examination-based methods (Zhang et al., 2023; Sriramanan et al., 2024; Du et al., 2024). Among these techniques, only token probability-based methods can be computed directly from the model’s output logits at no extra cost, making them well suited for inference-time intervention where efficiency is critical. Within this category, entropy is the most widely adopted metric for hallucination risk estimation (Kuhn et al., 2023; Kang et al., 2025). However, entropy fails in cases where the model produces confident but hallucinated responses (see Figure 3). To address this limitation, we propose *Visual Grounding Entropy* (VGE) to estimate hallucination risk for each token, which leverages visual grounding as a complementary signal to capture evidence mismatches beyond entropy (see Section 3.1 and Figure 4). Then, guided by VGE, **AdaVBoost** applies stronger visual attention boosting to high-risk tokens

and weaker boosting to low-risk tokens, enabling token-level adaptive intervention at each generation step. The computation of VGE is *lightweight*, ensuring **AdaVBoost** is computationally feasible and can be applied in practice with minimal overhead (see Section 4.5).

To deeply understand the failure cases of unfixable tokens in Figure 1b, we further examine generation behaviors from an alternative perspective by introducing textual suppression as a *complement* to visual boosting (see Figure 1c). Surprisingly, a large proportion of tokens that remain unfixable under visual boosting alone become non-hallucinatory when suppressing text input, suggesting that actively suppressing certain text tokens (e.g., text input) can serve as a complementary mechanism to visual boosting for effective hallucination mitigation. Motivated by this finding, **AdaVBoost** jointly boosts visual tokens and suppress text input tokens during each generation step. We provide ablation studies of textual suppression in Section 4.3.

We comprehensively evaluate **AdaVBoost** on state-of-the-art hallucination benchmarks, including CHAIR (Rohrbach et al., 2018), POPE (Li et al., 2023), AMBER (Wang et al., 2023), and SHR (Zhao et al., 2023b) and demonstrate its effectiveness in Section 4. Across LLaVA-NeXT-7B (Liu et al., 2024a), Qwen3-VL-8B (Bai et al., 2025), and InternVL3.5-8B (Wang et al., 2025), **AdaVBoost** consistently outperforms baseline methods by a notable margin, justifying the necessity to apply token-specific attention interventions during autoregressive generation.

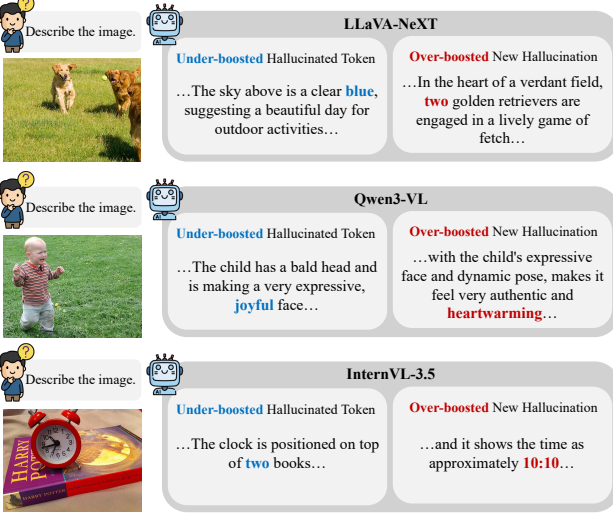


Figure 2. Examples of under-boosted and over-boosted hallucinated tokens in LLaVA-NeXT, Qwen3-VL and InternVL3.5.

The success of **AdaVBoost** can be summarized to three key factors: (1) The reliance on visual attention is inherently uneven across tokens during autoregressive generation, implying that effective hallucination mitigation requires token-specific visual interventions. (2) Existing visual boosting methods often rely on a pre-defined scaling factor, which can be either insufficient to suppress hallucinations at some generation steps or overly aggressive at others, leading to newly introduced hallucinations. By contrast, **AdaVBoost** adaptively determines *how much* attention to boost for each token, explicitly accounting for both under-boosted and over-boosted cases. (3) In addition to its effectiveness, **AdaVBoost** does not require additional training or extra forward passes, making it efficient and applicable to existing LVLMs in practical deployment scenarios.

2. Preliminary and Related Work

In this section, we first introduce the background of LVLMs, including their general structure and inference process. Then, we review visual attention boosting methods for hallucination mitigation in LVLMs.

LVLM structure. LVLMs typically consist of three core components: (i) a visual encoder, (ii) a modality connector for cross-modal alignment, and (iii) a *large language model* (LLM) backbone (Liu et al., 2024a; Bai et al., 2025; Wang et al., 2025). Given an input image I , the visual encoder extracts a sequence of visual representations, which are subsequently projected into the textual embedding space via the connector. This process produces N_i visual tokens $\mathbf{X}_i \in \mathbb{R}^{N_i \times d}$, where d denotes the hidden dimension. In parallel, the LLM tokenizer encodes the input text prompt into N_p textual tokens $\mathbf{X}_p \in \mathbb{R}^{N_p \times d}$. The visual and text tokens are

then concatenated to form the joint input sequence:

$$\mathbf{X} = [\mathbf{X}_i; \mathbf{X}_p] \in \mathbb{R}^{(N_i+N_p) \times d}.$$

which is fed into the LLM backbone. As autoregressive generation proceeds, the growing number of generated text tokens, in contrast to the fixed set of visual tokens, increasingly dominates the attention distribution, causing the model to place less emphasis on visual information and become more influenced by language priors, which in turn leads to hallucinations (Liu et al., 2024b; 2025).

LVLM inference. During inference, LVLMs generate a response sequence $R = \{y_1, \dots, y_L\}$ in an autoregressive manner. At each generation step t , the model predicts the next token conditioned on the input visual tokens \mathbf{X}_i , the input text tokens \mathbf{X}_p , and the previously generated tokens $\{y_1, \dots, y_{t-1}\}$. At each step, the influence of visual and textual information on next-token prediction is governed by the self-attention mechanism within the LLM. Specifically, within the l -th Transformer layer, causal self-attention is applied over the combined token sequence. For the newly generated token at step t , the query $\mathbf{Q}_l^{(t)}$ attends to all cached keys \mathbf{K}_l via:

$$\mathbf{A}_l^{(t)} = \text{Softmax} \left(\frac{\mathbf{Q}_l^{(t)} \mathbf{K}_l^\top}{\sqrt{d}} \right),$$

where $\mathbf{A}_l^{(t)}$ determines how the current token attends to visual tokens, text tokens, and previously generated tokens. Under this scheme, the attention weights assigned to visual tokens directly control the extent to which visual information influences generation at step t .

LVLM hallucination mitigation via visual attention boosting. In this paper, we mainly focus on visual attention boosting (Liu et al., 2024b; Yin et al., 2025; Xie et al., 2025; Zhao et al., 2025), which is a training-free paradigm that directly intervenes attention weights during the autoregressive generation process. Early efforts such as *Pay Attention to Image* (PAI) (Liu et al., 2024b) boost visual attention by uniformly amplifying attention weights of all visual tokens. Building on this idea, subsequent works have largely focused on *where* to boost visual attention by identifying visually relevant tokens or regions during generation. For example, *Visual Amplification Fusion* (VAF) (Yin et al., 2025) fuses visual signals into the attention process, thereby globally boosting visually grounded representations. *Temporal Attention Real-time Accumulation Connection* (TARAC) (Xie et al., 2025) further refines this direction by accumulating cross-modal attention patterns over time to identify modality-specific regions that warrant stronger visual emphasis. Similarly, *Vision-Guided Attention* (VGA) (Zhao et al., 2025) explicitly identifies visually relevant tokens using grounding-aware signals and guides

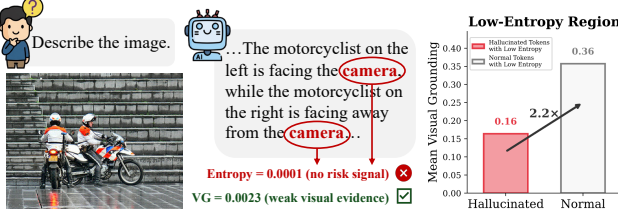


Figure 3. Left: An example where LLaVA-NeXT generates a hallucinated attribute (i.e., camera) with extremely low token entropy (i.e., extremely high confidence), indicating that using entropy alone sometimes fails to provide reliable risk signals. We use GPT-5-mini as a judge to decide if a token is hallucinated. This observation highlights a structural blind spot for confidence-based metrics (e.g., entropy) and motivates us to design a complementary signal beyond model confidence. Right: In the low-entropy region, we find that hallucinated tokens exhibit substantially weaker visual grounding (VG) scores than normal tokens, suggesting that VG can capture evidence mismatches that entropy fails to capture.

attention toward these selected tokens. Despite their differences in identifying *where* to boost, these methods typically rely on predefined or heuristic scaling strategies that apply a fixed guidance strength across generation steps.

3. AdaVBoost

In this paper, we identify a fundamental trade-off in existing visual attention boosting methods: a predefined scaling factor can be too weak at certain generation steps, leaving hallucinations unresolved, yet overly aggressive at others, introducing new hallucinations. Motivated by this observation, we propose **AdaVBoost**, a token-level visual attention boosting framework that moves beyond identifying *where* to boost and instead focuses on *how much* visual attention should be boosted at each generation step. This section first introduces *Visual Grounding Entropy* (VGE) as our hallucination risk estimator, and then presents the proposed adaptive visual attention boosting strategy together with textual suppression as a complementary mechanism. We summarize **AdaVBoost** in Algorithm 1.

3.1. Hallucination Risk Estimation

Entropy as a primary risk signal. Quantifying hallucination risk at the token level during autoregressive generation is central to our framework. In this paper, we focus on designing a lightweight and efficient approach that can be readily applied to existing LVLMs in practical deployment scenarios. There are several well-established paradigms to estimate hallucination risks, such as token probability-based methods (Takayama & Arase, 2019; Malinin & Gales, 2021), output consistency-based methods (Zhao et al., 2023a; Nikitin et al., 2024), and internal state examination-based methods (Zhang et al., 2023; Sriramanan et al., 2024; Du et al., 2024). Output consistency-based methods typically require multiple forward passes, resulting

in additional computational cost at inference time. Internal state examination-based methods, on the other hand, rely on accessing and storing intermediate representations at each generation step, which introduces non-trivial memory overhead. Among these techniques, only token probability-based methods can be computed directly from the model’s output logits at no extra cost, making them well suited for inference-time intervention where efficiency is critical. Within this category, entropy is the most widely adopted metric for hallucination risk estimation (Malinin & Gales, 2021; Kuhn et al., 2023; Kang et al., 2025). Formally, let \mathcal{V} denote the vocabulary, with size $V = |\mathcal{V}|$. At generation step t , given the output logits $\mathbf{z}_t \in \mathbb{R}^V$ from the language model, the predictive distribution is computed as:

$$p_t(v) = \text{Softmax}(\mathbf{z}_t)_v, \quad v \in \mathcal{V},$$

Then, the predictive entropy is defined as:

$$H_t = - \sum_{v \in \mathcal{V}} p_t(v) \log p_t(v).$$

Limitation of entropy. While entropy can serve as a reliable hallucination risk estimator when the model exhibits low confidence (Kuhn et al., 2023), it fails in cases where the model produces confident yet hallucinated responses. For example, as shown in Figure 3, LLaVA-NeXT generates an attribute prediction (i.e., “camera”) with extremely low token entropy, indicating high confidence in predicting the word “camera” following the phrase “is facing the”. However, the image provides no visual evidence to support the presence of a camera, and thus “camera” is a hallucinated token. This limitation motivates us to design an additional signal beyond entropy to capture such evidence mismatches.

Visual grounding as a complementary risk signal. To handle cases where the model produces confident but hallucinated responses, we further investigate the failure modes of entropy-based risk estimation. We find that hallucinations missed by entropy often arise from evidence mismatch rather than uncertainty. This observation motivates us to leverage *visual grounding* (VG) score as a complementary signal to entropy, which measures the alignment between generated tokens and visual evidence. Given an input image, we compute a vocabulary-level grounding vector during the pre-filling stage, where the image is encoded and processed once together with the input prompt before autoregressive decoding. This design allows the grounding vector to be obtained *without introducing any additional forward passes*, making it efficient for inference-time use. Formally, let \mathcal{I} denote the set of visual tokens, and let $\mathbf{h}_i \in \mathbb{R}^V$ denote the output logits associated with visual token $i \in \mathcal{I}$. The grounding vector $\mathbf{G} \in \mathbb{R}^V$ is defined as:

$$\mathbf{G}[v] = \max_{i \in \mathcal{I}} \text{Softmax}(\mathbf{h}_i)[v], \quad \forall v \in \mathcal{V}. \quad (1)$$

At generation step t , the predicted token $v_t^* = \arg \max_{v \in \mathcal{V}} v$ is assigned a grounding score $G_t = \mathbf{G}[v_t^*]$. Lower VG scores indicate weaker visual support for the generated token. For example, in Figure 3, since no “camera” is present in the image, the corresponding VG score is notably low, correctly reflecting the lack of visual evidence.

Effectiveness of VG in low-entropy region. To validate the effectiveness of VG, we conduct experiments in the low-entropy region, which is defined as tokens with normalized entropy below the median of all tokens (i.e., the bottom 50% by entropy). As shown in the right panel of Figure 3, the results demonstrate that the average visual grounding score is significantly lower for hallucinated tokens than for normal tokens, indicating that visual grounding provides a discriminative signal for identifying hallucinations when entropy is uninformative, i.e., when the model generates confident but hallucinated tokens.

Visual grounding entropy. However, VG is computed only once during the pre-filling stage and remains static throughout the entire generation process, making it insufficient to serve as a primary hallucination risk estimator. To this end, we propose *Visual Grounding Entropy* (VGE). Instead of replacing entropy, VGE leverages VG as a complementary risk signal to capture evidence mismatches that entropy fails to capture. Formally, at generation step t , we define VGE as a hallucination risk estimator that combines predictive uncertainty and visual grounding confidence. Let $\mathbf{z} \in \mathbb{R}^V$ denote the output logits over the vocabulary, and let $\mathbf{p} = \text{Softmax}(\mathbf{z})$. The normalized predictive entropy at generation step t is computed as:

$$\bar{H}_t = \frac{-\sum_{v \in \mathcal{V}} p_t(v) \log p_t(v)}{\log V}. \quad (2)$$

We then define the VGE as:

$$\text{VGE}_t = \alpha \cdot \bar{H}_t + (1 - \alpha) \cdot (1 - G_t), \quad (3)$$

where $\alpha \in [0, 1]$ is a balance coefficient that balances predictive uncertainty and visual grounding.

VGE vs entropy. As shown in Figure 4, VGE exhibits a substantially stronger and more consistent correlation with hallucinated tokens than entropy alone. In particular, entropy shows a non-monotonic behavior (e.g., Q5 yields noticeably more hallucinated tokens than Q6 and Q7), indicating that uncertainty alone can mis-rank hallucination risk at intermediate quantiles. In contrast, VGE produces a near-monotonic increase in hallucinated tokens from low to high quantiles, demonstrating that incorporating visual grounding enables a more reliable and well-ordered risk estimation across generation steps.

Comparison with hallucination detection methods. Although VGE correlates strongly with hallucinated tokens,

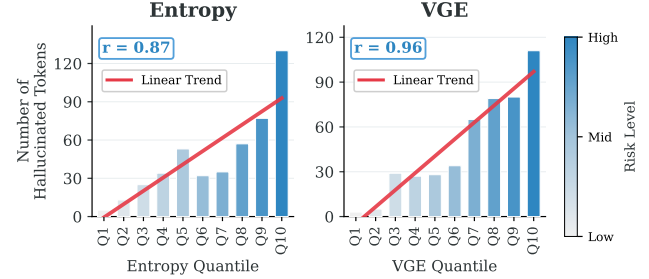


Figure 4. Comparison of entropy and VGE as hallucination risk estimators on LLaVA-NeXT. Each bar represents the number of hallucinated tokens within a signal quantile (Q1 = lowest, Q10 = highest). We use GPT-5-mini as a judge to decide if a token is hallucinated. Notably, VGE achieves a stronger correlation with the number of hallucinated tokens compared to entropy alone, demonstrating that incorporating visual grounding information helps identify hallucinated tokens that entropy misses.

we do not position it as a standalone hallucination detection method. Instead, VGE serves as a lightweight, token-level *risk signal* that can be computed on-the-fly during autoregressive generation, enabling adaptive attention boosting without additional forward passes or training. This design choice distinguishes our approach from prior detection methods (Zhao et al., 2023a; Zhang et al., 2023; Nikitin et al., 2024; Sriramanan et al., 2024; Du et al., 2024), which are typically used for post-hoc analysis rather than real-time hallucination risk estimation at token levels.

Comparison with VGA in visual grounding. Among existing methods, VGA explicitly leverages VG to guide attention allocation by identifying which visual tokens or regions should be boosted during generation (Zhao et al., 2025). By contrast, our method does not use VG to directly select or rank visual tokens. Instead, VG is incorporated into VGE as a complementary signal for estimating token-level hallucination risk, which subsequently controls how strongly visual attention is adaptively boosted at each generation step.

3.2. Adaptive Visual Attention Boosting

From VGE to boosting strength. Given VGE_t at generation step t , we first convert it into a normalized hallucination risk score that directly governs the strength of visual attention boosting. Specifically, we define the risk score as:

$$r_t = \min \left(\frac{\text{VGE}_t}{\gamma}, 1 \right), \quad (4)$$

where γ is the risk scale that controls the sensitivity of risk normalization. The resulting $r_t \in [0, 1]$ reflects the estimated hallucination risk score at step t , with larger values indicating the need for stronger visual boosting.

How much to boost. Based on the estimated hallucination risk score r_t , we compute a step-wise adaptive modulation factor that determines how much visual attention should be

boosted. The boosting strength at step t is defined as:

$$m_t = 1 + (m_{\text{vis}}^{\max} - 1) \cdot r_t, \quad (5)$$

where m_{vis}^{\max} denotes the maximum visual boosting factor. When $r_t = 0$, no visual boosting is applied (i.e., $m_t = 1$), preventing unnecessary intervention. As the risk increases, m_t grows smoothly, enabling stronger visual boosting to correct under-boosted hallucinations.

How to boost. We apply the adaptive boosting factor m_t to the pre-softmax self-attention scores associated with visual tokens during generation. Recall that at generation step t , within the ℓ -th Transformer layer, the attention scores (i.e., pre-softmax logits) for the newly generated token are given by $\mathbf{Z}_\ell^{(t)} \in \mathbb{R}^{1 \times (N_i + N_p + t - 1)}$. The corresponding attention weights are then computed as $\text{Softmax}(\mathbf{Z}_\ell^{(t)})$. Let \mathcal{I}_v denote the index set of visual tokens. For layers $\ell \in [L_s, L_e]$, we modulate the attention scores assigned to visual tokens as:

$$\tilde{\mathbf{Z}}_\ell^{(t)}[-1, \mathcal{I}_v] = m_t \cdot \mathbf{Z}_\ell^{(t)}[-1, \mathcal{I}_v]. \quad (6)$$

3.3. Textual Suppression

How much to suppress. Motivated by Figure 1c, we suppress the pre-softmax self-attention scores associated with text input tokens. Let \mathcal{I}_t denote the index set of text input tokens to be suppressed. For layers $\ell \in [L_s, L_e]$, we apply textual suppression by modulating the attention scores as:

$$\tilde{\mathbf{Z}}_\ell^{(t)}[-1, \mathcal{I}_t] = \frac{1}{m_{\text{txt}}^{\max}} \cdot \mathbf{Z}_\ell^{(t)}[-1, \mathcal{I}_t], \quad (7)$$

where m_{txt}^{\max} is the maximum textual suppression factor.

3.4. Final Attention Weights

The overall attention. After applying the above interventions, the final attention weights are obtained by applying the softmax function to the modulated attention scores:

$$\tilde{\mathbf{A}}_\ell^{(t)} = \text{Softmax}(\tilde{\mathbf{Z}}_\ell^{(t)}).$$

Through the softmax normalization, boosting visual token scores increases the probability mass allocated to visual evidence, while suppressing text input token scores correspondingly reduces the influence of language priors. As a result, the attention distribution for each generation step is adaptively reallocated between visual and textual modalities, enabling the model to rely more on visual information when hallucination risk is high and preventing over-dominance of textual context when such reliance is unnecessary.

4. Experiment

4.1. Experiment Setting

LVLM architectures. Following Xie et al. (2025), we evaluate the effectiveness of **AdaVBoost** on three representative LVLMs, covering different architectural paradigms:

Algorithm 1 AdaVBoost

Require: Image \mathbf{I} , text prompt \mathbf{x} , LVLM \mathcal{M}
Require: balance coefficient α , risk scale γ , maximum visual boosting factor m_{vis}^{\max} , maximum textual suppression factor m_{txt}^{\max} , layer range $[L_s, L_e]$
Ensure: Generated response $\mathbf{y} = (y_1, y_2, \dots, y_T)$

- 1: // *Prefilling stage*
- 2: $\mathbf{X}_i \leftarrow \text{VisualEncoder}(\mathbf{I})$ {Visual tokens}
- 3: $\mathbf{H}_0 \leftarrow \mathcal{M}.\text{Prefill}(\mathbf{X}_i, \mathbf{x})$ {Joint encoding}
- 4: $\mathbf{h}_i \leftarrow \text{LMHead}(\mathbf{H}_0^{(i)})$, $\forall i \in \mathcal{I}_v$
- 5: $\mathbf{G}[v] \leftarrow \max_{i \in \mathcal{I}_v} \text{Softmax}(\mathbf{h}_i)[v]$, $\forall v \in \mathcal{V}$ by Eq. (1)
- 6: $r_0 \leftarrow 0$ {Initialize risk}
- 7: // *Token-level adaptive boosting*
- 8: **for** $t = 1, \dots, T$ **do**
- 9: $m_t \leftarrow 1 + (m_{\text{vis}}^{\max} - 1) \cdot r_{t-1}$ by Eq. (5)
- 10: **for** $\ell = 1, \dots, L$ **do**
- 11: $\mathbf{Z}_\ell^{(t)} \leftarrow \text{PreSoftmaxAttentionScores}(\ell)$
- 12: **if** $L_s \leq \ell < L_e$ **then**
- 13: $\mathbf{Z}_\ell^{(t)}[-1, \mathcal{I}_v] \leftarrow \mathbf{Z}_\ell^{(t)}[-1, \mathcal{I}_v] \cdot m_t$ by Eq. (6)
- 14: $\mathbf{Z}_\ell^{(t)}[-1, \mathcal{I}_t] \leftarrow \mathbf{Z}_\ell^{(t)}[-1, \mathcal{I}_t] / m_{\text{txt}}^{\max}$ by Eq. (7)
- 15: **end if**
- 16: **end for**
- 17: $\mathbf{z}_t \leftarrow \text{LMHead}(\mathbf{h}_t^{(L)})$; $\mathbf{p}_t \leftarrow \text{Softmax}(\mathbf{z}_t)$;
- 18: $y_t \sim \mathbf{p}_t$; Append y_t to \mathbf{y}
- 19: // *Update hallucination risk*
- 20: $\bar{H}_t \leftarrow -\sum_{v \in \mathcal{V}} p_t(v) \log p_t(v) / \log |\mathcal{V}|$ by Eq. (2)
- 21: $v_t^* \leftarrow \arg \max_{v \in \mathcal{V}} \mathbf{z}_t[v]$; $G_t \leftarrow \mathbf{G}[v_t^*]$
- 22: $\text{VGE}_t \leftarrow \alpha \cdot \bar{H}_t + (1 - \alpha) \cdot (1 - G_t)$ by Eq. (3)
- 23: $r_t \leftarrow \min(1, \text{VGE}_t / \gamma)$ by Eq. (4)
- 24: **end for**
- 25: **Return** \mathbf{y}

LLaVA-NeXT-7B (Liu et al., 2024a), Qwen3-VL-8B (Bai et al., 2025), and InternVL3.5-8B (Wang et al., 2025).

Hallucination benchmarks. **AdaVBoost** is evaluated on four state-of-the-art hallucination benchmarks: CHAIR (Rohrbach et al., 2018), SHR (Zhao et al., 2023b), POPE (Li et al., 2023) and AMBER (Wang et al., 2023). CHAIR and SHR evaluate hallucinations in generative tasks (e.g., describing images), POPE focuses on hallucination evaluation in discriminative tasks (e.g., answering yes/no questions about object presence in an image), and AMBER is a hybrid benchmark covering both generative and discriminative tasks. We provide detailed descriptions of these benchmarks and their evaluation metrics in Appendix B.1.

Baselines. Following Zhao et al. (2025), we use three visual attention boosting methods for comparison: PAI (Liu et al., 2024b), VAF (Yin et al., 2025) and VGA (Zhao et al., 2025). We provide detailed configurations of these methods in Appendix B.2. TARAC (Xie et al., 2025) is also a relevant baseline. However, since its official implementation is not publicly available yet, we do not include it in our comparison to avoid potential reproduction discrepancies.

Implementation details. For each LVLM, we specify a model-specific set of hyperparameters, which is then kept

Table 1. Results on CHAIR benchmark. We report the best result in **bold**.

Method	LLaVA-NeXT			Qwen3-VL			InternVL3.5		
	CHAIRs ↓	CHAIRi ↓	F1 ↑	CHAIRs ↓	CHAIRi ↓	F1 ↑	CHAIRs ↓	CHAIRi ↓	F1 ↑
Vanilla	33.80	8.46	71.44	58.80	10.57	75.29	41.40	10.80	74.71
PAI	39.60	10.06	72.15	53.60	10.47	74.95	45.60	11.81	74.98
VAF	36.40	9.14	71.66	53.60	9.75	75.15	42.20	11.00	74.58
VGA	32.40	9.90	71.26	58.40	10.50	74.73	44.20	11.57	74.68
Ours	28.80	7.66	71.18	46.00	8.38	75.22	34.40	9.34	75.32

Table 2. Results on SHR benchmark. We use GPT-5-mini as a judge. We report the best result in **bold**.

Method	LLaVA-NeXT				Qwen3-VL				InternVL3.5			
	HSR ↓	HWR ↓	HSPI ↓	HWPI ↓	HSR ↓	HWR ↓	HSPI ↓	HWPI ↓	HSR ↓	HWR ↓	HSPI ↓	HWPI ↓
Vanilla	31.40	32.80	2.71	48.19	23.10	24.70	3.94	72.62	26.10	29.70	2.15	37.73
PAI	32.80	34.40	2.79	49.96	26.20	28.50	3.87	72.21	24.30	26.90	1.85	33.40
VAF	31.90	33.50	2.77	49.30	24.00	25.70	4.09	75.78	25.90	29.20	2.13	37.01
VGA	31.10	32.70	2.69	47.93	22.70	24.30	3.88	71.64	25.40	28.70	2.08	36.22
Ours	30.70	32.60	2.69	45.14	22.10	23.30	3.51	69.84	22.40	25.70	1.63	26.74

fixed across all benchmarks. For LLaVA-NeXT-7B, we set the balance coefficient α to 0.5, risk scale γ to 0.5, the maximum visual boosting factor m_{vis}^{\max} to 1.1 and the maximum textual suppression factor m_{txt}^{\max} to 1.7. For Qwen3-VL-8B, we set α to 0.6, γ to 0.6, m_{vis}^{\max} to 1.3 and m_{txt}^{\max} to 1.3. For InternVL3.5-8B, we set α to 0.8, γ to 0.7, m_{vis}^{\max} to 1.3 and m_{txt}^{\max} to 1.6. We provide sensitivity analysis for these hyperparameters in Section 4.4. Following Zhao et al. (2025), we set the starting layer for LLaVA-NeXT-7B to 0 and ending layer to 16. For Qwen3-VL-8B and InternVL3.5-8B, we set the starting layer to 4 and ending layer for 16.

4.2. Main Result

CHAIR evaluation. The experimental results on the CHAIR benchmark are reported in Table 1. Across all three LVLMs, **AdaVBoost** consistently achieves the best *CHAIRs* and *CHAIRi* scores and consistently outperforms baseline methods by a notable margin. For example, **AdaVBoost** achieves at least a reduction of 3.60, 7.60 and 7.00 on *CHAIRs* across LLaVA-NeXT, Qwen3-VL and InternVL3.5, indicating that **AdaVBoost** substantially reduces hallucinations across all models, where both sentence-level and instance-level errors are markedly decreased compared to baseline methods. More importantly, these gains are obtained without sacrificing generation quality, as the *F1* scores remain comparable to or slightly better than the original model. Overall, the results demonstrate that **AdaVBoost** effectively mitigates visual hallucinations while preserving strong discriminative performance.

SHR evaluation. The experimental results on the SHR benchmark are reported in Table 2, where GPT-5-mini is used as the judge (we provide detailed prompt instruction in Figure 8). Across all three LVLMs, **AdaVBoost** consistently achieves the best hallucination mitigation on all

four SHR metrics, including *HSR*, *HWR*, *HSPI*, and *HWPI*, demonstrating clear and consistent improvements over baseline methods. In particular, **AdaVBoost** yields substantial reductions in both sentence-level and word-level hallucinations, with especially pronounced gains on InternVL3.5, where all four metrics are significantly improved.

AMBER evaluation. The experimental results on the AMBER benchmark are reported in Table 3. AMBER jointly evaluates hallucination severity and content coverage, providing a more balanced assessment of generation quality. Across all three LVLMs, **AdaVBoost** consistently achieves the lowest hallucination rate (i.e., *Hal*) while incurring only a marginal reduction in *Cover*, resulting in a favorable trade-off between hallucination mitigation and semantic coverage. Notably, **AdaVBoost** consistently reduces other metrics such as *CHAIR* and *Cog* across all models. We provide full results of AMBER (including the discriminative task) in Appendix C.1. We observe that the advantages of **AdaVBoost** are relatively small on discriminative tasks than on generative ones. A key reason is that discriminative tasks usually require predicting a single, closed-form token (e.g., a binary answer), leaving limited room for adaptive visual attention boosting during the autoregressive generation. As a result, model behavior in these settings resembles a one-shot visual classification process, where performance is primarily governed by the capability of original model.

POPE evaluation. The results on the POPE benchmark are summarized in Appendix C.2, where performance is reported as the average across three VQA datasets, including MSCOCO, A-OKVQA, and GQA. Similar to the results of AMBER on discriminative tasks, the improvements brought by **AdaVBoost** on discriminative tasks are relatively modest. This is expected, as POPE requires predicting a single, closed-form answer (e.g., a binary response). Im-

Table 3. Results on AMBER benchmark. We report the best result in **bold**.

Method	LLaVA-NeXT				Qwen3-VL				InternVL3.5			
	CHAIR ↓	Cover ↑	Hal ↓	Cog ↓	CHAIR ↓	Cover ↑	Hal ↓	Cog ↓	CHAIR ↓	Cover ↑	Hal ↓	Cog ↓
Vanilla	7.83	63.87	49.20	4.33	7.66	73.59	59.24	3.75	7.49	74.24	62.20	5.95
PAI	8.29	64.74	50.90	4.43	8.23	74.11	63.39	3.50	8.51	74.88	66.00	5.29
VAF	7.64	63.24	47.41	3.70	7.41	72.75	56.64	3.38	7.30	71.64	53.20	3.99
VGA	7.65	62.39	40.74	3.59	7.97	73.32	60.31	3.34	7.36	73.99	62.09	5.49
Ours	6.97	61.21	39.85	3.41	6.74	72.12	51.30	3.00	6.50	72.30	50.24	2.78

portantly, across all three LVLMs and evaluation settings, **AdaVBoost** preserves the original model utility, achieving accuracy and *F1* scores that are comparable to the vanilla baselines. These results indicate that **AdaVBoost** does not compromise discriminative capabilities while effectively mitigating hallucinations during autoregressive generation.

4.3. Ablation Study

Ablation study on method components. We conduct an ablation study on the effectiveness of each individual component in our method (see Table 6 in Appendix C.3). Both textual suppression and visual boosting lead to consistent reductions in hallucination metrics across all three LVLMs, indicating that each component is effective. In particular, visual boosting yields the most significant improvements on both *CHAIRs* and *CHAIRi*, highlighting the importance of strengthening visual grounding during generation.

Ablation study on textual suppression scope. We also conduct an ablation study on the scope of textual suppression (see Table 7 in Appendix C.3). Notably, suppressing all text tokens leads to the lowest hallucination scores but incurs a noticeable drop in *F1*, indicating overly conservative generation. In contrast, restricting suppression to text input tokens achieves a better balance, consistently reducing hallucinations while preserving generation quality across all three LVLMs. These results suggest that limiting textual suppression to the input side is both effective and preferable.

4.4. Sensitivity Analysis

We conduct a comprehensive sensitivity analysis in Appendix C.4. For the balance coefficient α and the risk scale γ , we observe stable and consistent performance trends across a wide range of values for both hyperparameters. Importantly, across all tested settings, **AdaVBoost** consistently outperforms the baselines (see Tables 8 and 9). For the maximum visual boosting factor m_{vis}^{\max} and the maximum textual suppression factor m_{txt}^{\max} , we observe that excessively large values of either factor can lead to performance degradation, particularly for Qwen3-VL (see Tables 10 and 11). This behavior is expected, as overly aggressive visual boosting or text suppression may distort the original attention distribution, causing the model to overemphasize or underutilize certain modalities. This phenomenon

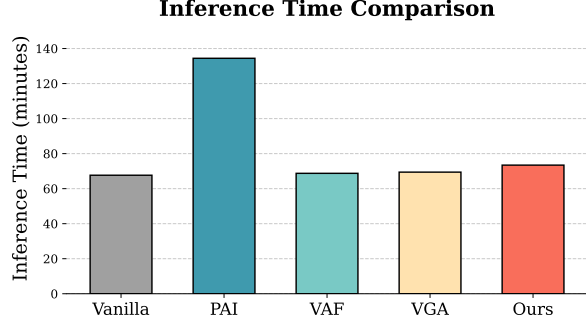


Figure 5. Inference time comparison of different methods on the CHAIR benchmark using LLaVA-NeXT-7B.

is consistent with observations reported in Liu et al. (2024b). Notably, within a moderate range of values, our method consistently achieves strong hallucination reduction while maintaining stable *F1* scores, indicating that the method is effective and robust under reasonable boosting strengths.

4.5. Inference Efficiency

As shown in Figure 5, **AdaVBoost** incurs only a marginal inference-time overhead compared to the vanilla model, while remaining substantially more efficient than PAI, which requires an additional forward pass.

5. Conclusion

We identify a fundamental limitation of prior visual boosting methods, where a fixed scaling factor fails to adapt to the varying hallucination risk associated with each token across generation steps. To address this issue, we propose **AdaVBoost**, a token-level adaptive visual attention boosting framework guided by *Visual Grounding Entropy* (VGE), which dynamically adjusts the boosting strength according to the estimated risk at each generation step. By selectively strengthening visual attention for high-risk tokens and applying milder boosting for low-risk ones, **AdaVBoost** effectively mitigates hallucinations without compromising generation quality. Extensive experiments across multiple LVLMs and hallucination benchmarks demonstrate that **AdaVBoost** achieves consistent and robust improvements over existing approaches. We hope this simple yet effective framework highlights the importance of risk-aware and adaptive interventions to improve the reliability of LVLMs.

Impact Statement

This work on mitigating hallucinations in LVLMs raises important considerations regarding the reliability and responsible deployment of multimodal AI systems. We have taken care to evaluate our method using widely adopted public benchmarks and established evaluation protocols to ensure fair and transparent comparison with prior approaches. Our experiments span multiple model architectures and hallucination benchmarks, providing a comprehensive assessment of the method’s effectiveness and robustness. We also consider the broader impact of this work. By reducing hallucinations during autoregressive generation, the proposed framework has the potential to improve the factual reliability and trustworthiness of LVLMs in real-world applications, such as visual question answering and image-grounded content generation. At the same time, our method operates entirely at inference time and does not introduce additional training data or external supervision, which helps limit the risk of unintended bias amplification. We hope this work contributes to the development of more reliable multimodal systems and encourages further research into risk-aware and adaptive mechanisms for safe AI generation.

References

Bai, S., Cai, Y., Chen, R., Chen, K., Chen, X.-H., Cheng, Z., Deng, L., Ding, W., Fang, R., Gao, C., Ge, C., Ge, W., Guo, Z., Huang, Q., Huang, J., Huang, F., Hui, B., Jiang, S., Li, Z., Li, M., Li, M., Li, K., Lin, Z., Lin, J., Liu, X., Liu, J., Liu, C., Liu, Y., Liu, D., Liu, S., Lu, D., Luo, R., Lv, C., Men, R., Meng, L. Y., Ren, X., yi Ren, X., Song, S., Sun, Y.-C., Tang, J., Tu, J., Wan, J., Wang, P., Wang, P., Wang, Q., Wang, Y., Xie, T., Xu, Y., Xu, H., Xu, J., Yang, Z., Yang, M., Yang, J., Yang, A., Yu, B., Zhang, F., Zhang, H., Zhang, X., Zheng, B., Zhong, H., Zhou, J., Zhou, F., Zhou, J., Zhu, Y., and Zhu, K. Qwen3-vl technical report. *ArXiv*, abs/2511.21631, 2025.

Bai, Z., Wang, P., Xiao, T., He, T., Han, Z., Zhang, Z., and Shou, M. Z. Hallucination of multimodal large language models: A survey. *ArXiv*, abs/2404.18930, 2024.

Du, X., Xiao, C., and Li, Y. Haloscope: Harnessing unlabeled llm generations for hallucination detection. *NeurIPS*, 2024.

Huang, L., Yu, W., Ma, W., Zhong, W., Feng, Z., Wang, H., Chen, Q., Peng, W., Feng, X., Qin, B., and Liu, T. A survey on hallucination in large language models: Principles, taxonomy, challenges, and open questions. *ACM Transactions on Information Systems*, 2023.

Huang, Q., wen Dong, X., Zhang, P., Wang, B., He, C., Wang, J., Lin, D., Zhang, W., and Yu, N. H. Opera: Alleviating hallucination in multi-modal large language models via over-trust penalty and retrospection-allocation. *CVPR*, 2024.

Hudson, D. A. and Manning, C. D. Gqa: A new dataset for real-world visual reasoning and compositional question answering. *CVPR*, 2019.

Huo, F., Xu, W., Zhang, Z., Wang, H., Chen, Z., and Zhao, P. Self-introspective decoding: Alleviating hallucinations for large vision-language models. *ArXiv*, abs/2408.02032, 2024.

Jiang, C., Xu, H., Dong, M., Chen, J., Ye, W., Yan, M., Ye, Q., Zhang, J., Huang, F., and Zhang, S. Hallucination augmented contrastive learning for multimodal large language model. *CVPR*, 2024.

Kang, S., Bakman, Y. F., Yaldiz, D. N., Buyukates, B., and Avestimehr, A. S. Uncertainty quantification for hallucination detection in large language models: Foundations, methodology, and future directions. *ArXiv*, abs/2510.12040, 2025.

Krishna, R., Zhu, Y., Groth, O., Johnson, J., Hata, K., Kravitz, J., Chen, S., Kalantidis, Y., Li, L.-J., Shamma, D. A., Bernstein, M. S., and Fei-Fei, L. Visual genome: Connecting language and vision using crowdsourced dense image annotations. *IJCV*, 2016.

Kuhn, L., Gal, Y., and Farquhar, S. Semantic uncertainty: Linguistic invariances for uncertainty estimation in natural language generation. *ICLR*, 2023.

Leng, S., Zhang, H., Chen, G., Li, X., Lu, S., Miao, C., and Bing, L. Mitigating object hallucinations in large vision-language models through visual contrastive decoding. *CVPR*, 2024.

Li, Y., Du, Y., Zhou, K., Wang, J., Zhao, W. X., and rong Wen, J. Evaluating object hallucination in large vision-language models. In *EMNLP*, 2023.

Lin, T.-Y., Maire, M., Belongie, S. J., Hays, J., Perona, P., Ramanan, D., Dollár, P., and Zitnick, C. L. Microsoft coco: Common objects in context. In *ECCV*, 2014.

Liu, C., Xu, Z., Wei, Q., Wu, J., Zou, J. Y., Wang, X. E., Zhou, Y., and Liu, S. More thinking, less seeing? assessing amplified hallucination in multimodal reasoning models. *ArXiv*, abs/2505.21523, 2025.

Liu, H., Li, C., Li, Y., and Lee, Y. J. Improved baselines with visual instruction tuning. *CVPR*, 2023.

Liu, H., Li, C., Li, Y., Li, B., Zhang, Y., Shen, S., and Lee, Y. J. Llava-next: Improved reasoning, ocr, and world knowledge, 2024a. URL <https://llava-vl.github.io/blog/2024-01-30-llava-next/>.

Liu, S., Zheng, K., and Chen, W. Paying more attention to image: A training-free method for alleviating hallucination in lvlms. *ECCV*, 2024b.

Malinin, A. and Gales, M. J. F. Uncertainty estimation in autoregressive structured prediction. In *International Conference on Learning Representations*, 2021.

Nikitin, A., Kossen, J., Gal, Y., and Marttinen, P. Kernel language entropy: Fine-grained uncertainty quantification for llms from semantic similarities. *ArXiv*, abs/2405.20003, 2024.

OpenAI. Gpt-5 mini model documentation, 2025. URL <https://platform.openai.com/docs/models/gpt-5-mini>. OpenAI API model card.

Rohrbach, A., Hendricks, L. A., Burns, K., Darrell, T., and Saenko, K. Object hallucination in image captioning. In *EMNLP*, 2018.

Schwenk, D., Khandelwal, A., Clark, C., Marino, K., and Mottaghi, R. A-okvqa: A benchmark for visual question answering using world knowledge. In *ECCV*, 2022.

Sriramanan, G., Bharti, S., Sadasivan, V. S., Saha, S., Katikonda, P., and Feizi, S. Llm-check: Investigating detection of hallucinations in large language models. *NeurIPS*, 2024.

Sun, Z., Shen, S., Cao, S., Liu, H., Li, C., Shen, Y., Gan, C., Gui, L., Wang, Y., Yang, Y., Keutzer, K., and Darrell, T. Aligning large multimodal models with factually augmented RLHF. In *ACL*, 2024.

Takayama, J. and Arase, Y. Relevant and informative response generation using pointwise mutual information. *Proceedings of the First Workshop on NLP for Conversational AI*, 2019.

Wang, J., Wang, Y., Xu, G., Zhang, J., Gu, Y., Jia, H., Xu, H., Yan, M., Zhang, J., and Sang, J. An llm-free multi-dimensional benchmark for mllms hallucination evaluation. *ArXiv*, abs/2311.07397, 2023.

Wang, W., Gao, Z., Gu, L., Pu, H., Cui, L., Wei, X., Liu, Z., Jing, L., Ye, S., Shao, J., Wang, Z., Chen, Z., Zhang, H., Yang, G., Wang, H., Wei, Q., Yin, J., Li, W., Cui, E., Chen, G., Ding, Z., Tian, C., Wu, Z., Xie, J., Li, Z., Yang, B., Duan, Y., Wang, X., Hao, H., Li, S., Zhao, X., Duan, H., Deng, N., Fu, B., He, Y., Wang, Y., He, C., Shi, B., He, J., Xiong, Y., Lv, H., Wu, L., Shao, W., Zhang, K., Deng, H., Qi, B., Qi, B., Guo, Q., Zhang, W., Gu, Y., Ouyang, W., Wang, L., Dou, M., Zhu, X., Lu, T., Lin, D., Dai, J., Zhou, B., Su, W., Chen, K., Qiao, Y., Wang, W., and Luo, G. Internvl3.5: Advancing open-source multimodal models in versatility, reasoning, and efficiency. *ArXiv*, abs/2508.18265, 2025.

Wang, X., Pan, J., Ding, L., and Biemann, C. Mitigating hallucinations in large vision-language models with instruction contrastive decoding. In *ACL*, 2024.

Xiao, X., Wu, B., Wang, J., Li, C., Zhou, X., and Guo, H. Seeing the image: Prioritizing visual correlation by contrastive alignment. In *NeurIPS*, 2024.

Xie, C., Liu, T., Jiang, L., Zeng, Y., Guo, J., Shen, Y., Huang, W., Li, J., and Xu, X. Tarac: Mitigating hallucination in lvlms via temporal attention real-time accumulative connection. *ICML*, 2025.

Xing, Y., Li, Y., Laptev, I., and Lu, S. Mitigating object hallucination via concentric causal attention. In *NeurIPS*, 2024.

Yin, H., Si, G., and Wang, Z. Clearsight: Visual signal enhancement for object hallucination mitigation in multi-modal large language models. *CVPR*, 2025.

Yue, Z., Zhang, L., and Jin, Q. Less is more: Mitigating multimodal hallucination from an EOS decision perspective. In *ACL*, 2024.

Zhang, T., Qiu, L., Guo, Q., Deng, C., Zhang, Y., Zhang, Z., Zhou, C., Wang, X., and Fu, L. Enhancing uncertainty-based hallucination detection with stronger focus. In *EMNLP*, 2023.

Zhao, H., Si, S., Chen, L., Zhang, Y., Sun, M., Zhang, M., and Chang, B. Looking beyond text: Reducing language bias in large vision-language models via multi-modal dual-attention and soft-image guidance. *ArXiv*, abs/2411.14279, 2024.

Zhao, J., Zhang, F., Sun, X., Feng, C., and Tan, Z. Tell model where to look: Mitigating hallucinations in mllms by vision-guided attention. *ArXiv*, abs/2511.20032, 2025.

Zhao, Y., Yan, L., Sun, W., Xing, G., Meng, C., Wang, S., Cheng, Z., Ren, Z., and Yin, D. Knowing what llms do not know: A simple yet effective self-detection method. *ArXiv*, abs/2310.17918, 2023a.

Zhao, Z., Wang, B., Ouyang, L., wen Dong, X., Wang, J., and He, C. Beyond hallucinations: Enhancing lvlms through hallucination-aware direct preference optimization. *ArXiv*, abs/2311.16839, 2023b.

A. Analysis of Hallucination in Motivation Experiments

A.1. How to Measure Hallucination: GPT-5-mini as a Judge vs. Rule-based Metrics

Accurately evaluating hallucinations in LVLMs depends critically on how hallucination is defined under the target task. Our motivation experiments as well as the problem setting of our paper focus on open-ended prompts such as “*Describe the image*”, where models are encouraged to generate natural, narrative-style descriptions rather than strictly enumerating annotated visual entities. In this paper, we mainly use GPT-5-mini as a judge to decide whether a token is hallucinated (we provide the prompt template in Figure 8). Previous hallucination evaluation (e.g., AMBER) mainly uses rule-based metrics to flag tokens not explicitly grounded in provided annotations. While effective for closed-set or object-centric evaluation, we observe that such rule-based metrics tend to over-penalize benign narrative elaborations in open-ended image description tasks, leading to an inflated false negative rate.

We illustrate this limitation with two representative examples (see Figures 6 and 7). In the first example, the rule-based metric flags tokens such as *rocks* and *clouds* as hallucinations solely because they are absent from the provided annotations. However, a closer inspection of the generated description reveals that the model refers to *small rocks* scattered on the beach and a sky *devoid of any clouds*, both of which are accurate and scene-consistent visual descriptions rather than hallucinations. This highlights a fundamental limitation of rule-based evaluation, which cannot assess contextual correctness beyond annotation matching. In contrast, GPT-5-mini does not treat these tokens as hallucinations and instead identifies a more salient and semantically critical error: the model describes the child as being dressed in a *blue and white striped shirt*, whereas the child’s upper body is in fact bare.

In the second example, the rule-based metrics penalizes *building* by incorrectly interpreting *building* as a hallucinated noun. However, in the original sentence (“*used for building sandcastles*”), *building* clearly functions as a verb describing the typical use of the bucket, rather than introducing a new visual entity. This illustrates a second limitation of rule-based evaluation, namely its inability to disambiguate linguistic roles and semantic functions beyond surface-level token matching. As a result, harmless commonsense explanations are mistakenly classified as hallucinations. In contrast, GPT-5-mini correctly avoids this pitfall by recognizing the verb usage of *building* and does not penalize such explanatory narration.

Importantly, GPT-5-mini as a judge distinguishes harmful hallucinations from harmless narrative expansions, aligning more closely with human perception of factual inconsistency in open-ended descriptions. Therefore, we adopt GPT-5-mini as the hallucination judge in our motivation experiments, as it provides a more semantically grounded and task-aligned evaluation compared to annotation-dependent rule-based metrics. At the same time, we acknowledge that using LLMs as judges is not a perfect solution for hallucination evaluation, as LLMs themselves may also exhibit hallucinations. More broadly, how to reliably measure hallucination remains an open and challenging problem. Nevertheless, given the limitations of annotation-dependent rule-based metrics in open-ended generation settings, we argue that strong contemporary models such as GPT-5-mini are more likely to provide accurate and semantically meaningful judgments than purely rule-based approaches. In particular, GPT-5-mini is better equipped to reason about contextual plausibility and linguistic semantics, which are critical for distinguishing harmful hallucinations from benign narrative elaborations.



Describe the image.

"In the image, a young child is the main subject, captured in a moment of pure joy and freedom. The child, dressed in a blue and **white striped shirt** and black shorts, is running on a sandy beach. The child's arms are outstretched, as if embracing the world around them. Their feet are sinking into the soft sand, leaving behind a trail of footprints. The beach itself is a beautiful blend of light and dark sand, with small **rocks** scattered across the surface. The child is moving towards the left side of the image, their body leaning into the run. In the background, the vast expanse of the ocean stretches out, its surface a deep blue. A few small waves are visible, breaking gently on the shore. Above it all, the sky is a clear blue, devoid of any **clouds**. The image is a snapshot of a perfect day at the beach, filled with sunshine, sand, and the endless blue of the ocean. It's a moment of pure childhood delight, captured in one single frame."

Hallucinated tokens judged by GPT-5-mini: “white”, “striped”, “shirt”

Hallucinated tokens judged by rule-based metric: “rocks”, “clouds”

Figure 6. An example of GPT-5-mini as a judge vs. rule-based metrics for hallucination detection.

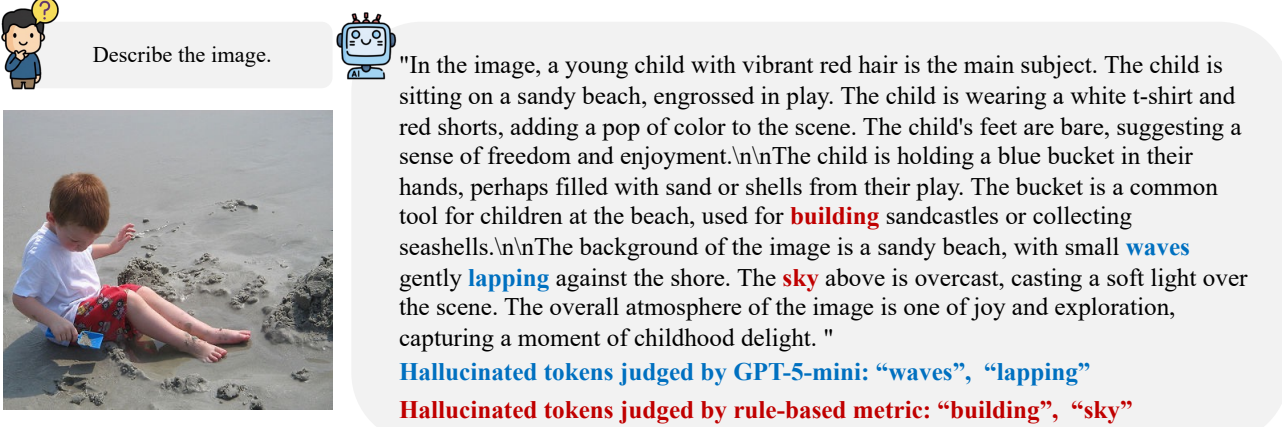


Figure 7. An example of GPT-5-mini as a judge vs. rule-based metrics for hallucination detection.

A.2. Definition of Under-boosted Hallucinated Tokens vs. Over-boosted Hallucinated Tokens

In the motivation analysis (see Figure 1), we aim to characterize how visual boosting affects hallucinations at the token level by distinguishing (i) hallucinations newly *introduced* by boosting, (ii) hallucinations that *remain* after boosting, and (iii) among the remaining ones, those that can be *resolved* by further increasing the boosting strength.

Token-level hallucination sets. Let $\mathcal{H}_{\text{base}}$ and $\mathcal{H}_{\text{boost}}$ denote the sets of hallucinated tokens identified in the BASELINE and BOOST responses, respectively. We first form the candidate set of “newly appearing” hallucinated tokens:

$$\mathcal{C} = \mathcal{H}_{\text{boost}} \setminus \mathcal{H}_{\text{base}}.$$

Derived vs. truly new hallucinations. A key ambiguity is that a token in \mathcal{C} may not represent a truly new hallucination; it can be a *derived* hallucination that replaces an already-hallucinated token in the baseline at the same semantic position (e.g., changing one incorrect attribute to another). To disambiguate this, we use GPT-5-mini to classify each token in \mathcal{C} as either **DERIVED** or **NEW**, following the prompt we provided in Figure 9. We denote the derived subset as $\mathcal{D} \subseteq \mathcal{C}$ and the truly new subset as $\mathcal{N} = \mathcal{C} \setminus \mathcal{D}$.

Over-boosted hallucinated tokens. We define *over-boosted hallucinated tokens* as hallucinations that are *introduced by visual boosting* and are *not derived* from any baseline hallucination:

$$\mathcal{H}_{\text{over}} \triangleq \mathcal{N}.$$

Intuitively, $\mathcal{H}_{\text{over}}$ captures genuinely new, unsupported content that emerges after boosting, rather than a mere mutation of an existing hallucination.

Remaining hallucinations. We group together (i) hallucinations that persist from baseline and (ii) hallucinations that are derived mutations of baseline hallucinations, and refer to them as *remaining hallucinations*:

$$\mathcal{H}_{\text{rem}} \triangleq (\mathcal{H}_{\text{boost}} \cap \mathcal{H}_{\text{base}}) \cup \mathcal{D}.$$

This set represents hallucinated semantics that were already present in the baseline response and are not eliminated by the current boosting strength, possibly with altered surface forms.

Under-boosted hallucinated tokens. Finally, we define *under-boosted hallucinated tokens* as the subset of remaining hallucinations that can be resolved by increasing the visual boosting strength. Concretely, consider a stronger boosting setting (denoted BOOST^+) with a higher boosting magnitude (in the motivation experiment, we set the maximum scaling factor to 1.6), and let $\mathcal{H}_{\text{boost}^+}$ be its hallucinated-token set. A remaining hallucinated token is said to be *resolved* if it becomes non-hallucinatory under stronger boosting, i.e., it no longer belongs to the hallucinated-token set. We then define:

$$\mathcal{H}_{\text{under}} \triangleq \{ h \in \mathcal{H}_{\text{rem}} \mid h \notin \mathcal{H}_{\text{boost}^+} \}.$$

Intuitively, $\mathcal{H}_{\text{under}}$ corresponds to hallucinations that the current boosting strength fails to correct, but which are fixable by further strengthening visual grounding.

A.3. Prompt Templates for GPT-5-mini



JUDGE_PROMPT = """You are an expert at detecting hallucinations in image descriptions.

Given:

- An image
- A question: "{query}"
- A model's response: "{response}"

Your task: Identify ALL hallucinated WORDS (nouns, adjectives, verbs, numbers) in the response.

A hallucinated word is defined as:

1. A clearly non-existent object/person. A word that refers to an object, person, or scene element that the image provides strong evidence does not exist. (e.g., "dog", "car", "woman" when the image clearly shows none).
2. A provably wrong attribute. A word that assigns an attribute to a visible entity that is visually contradicted with high confidence, including:
 1. color (e.g., "red" when the object is clearly blue)
 2. number/count (e.g., "three" when there are clearly two)
 3. shape/material/type when the image provides unambiguous evidence
3. A visually impossible action or state. A word that describes an action, interaction, or state that is clearly incompatible with the image, based on physical or temporal evidence. (e.g., "running" when the person is clearly sitting still).

DO NOT mark as hallucinated for:

1. Function words (a, the, of, in, on, is, are, etc.), which do not express visual content.
2. Words that are supported or plausible given the image, even if they are not mentioned in annotations.
3. Words that are visually uncertain or ambiguous. If the image does not provide enough evidence to confidently confirm or deny the word, do NOT mark it as hallucinated.

Output ONLY a JSON object with individual hallucinated words:

{ "hallucinated_words": ["word1", "word2", ...] }

If there are no hallucinations, output:

{ "hallucinated_words": [] }

Be precise - only output the specific words that satisfy the definition of hallucination, not entire phrases."""

Figure 8. Prompt for GPT-5-mini to decide whether a word is hallucinated.



JUDGE_PROMPT = """"You are an expert at analyzing text differences to identify hallucination patterns.

Task

Compare two responses (BASELINE and BOOST) describing the same image. Both responses may contain hallucinated words.

Your job is to classify each hallucinated word in the BOOST response that was NOT hallucinated in BASELINE:

1. ****DERIVED****: The word replaced or evolved from a hallucinated word in BASELINE. They describe the same semantic role/position in the sentence, just with a different incorrect word.

- Example: BASELINE has "cat" (HAL), BOOST has "dog" (HAL) → "dog" is DERIVED from "cat"
- Example: BASELINE has "red car" (red is HAL), BOOST has "blue car" (blue is HAL) → "blue" is DERIVED from "red"

2. ****NEW****: The word describes something that was either:

- Correctly described (or not mentioned) in BASELINE, but incorrectly described in BOOST
- A completely new hallucinated concept not present in BASELINE at all
- Example: BASELINE says "a person walking", BOOST says "a person walking with a dog" where "dog" is HAL → "dog" is NEW

Input Format

- BASELINE response and its hallucinated words
- BOOST response and its hallucinated words
- CANDIDATE words: HAL words in BOOST that are NOT in BASELINE's HAL list (these need classification)

Important Rules

- A word is DERIVED only if it clearly replaces another hallucinated word in the same semantic position
- If unsure, classify as NEW (be conservative)
- The same baseline HAL word can only be the source for ONE derived word
- Consider sentence structure and meaning, not just word proximity

"""

Figure 9. Prompt for GPT-5-mini to decide whether a hallucinated word is over-boosted or derived from a previous hallucinated token.

B. Detailed Experiment Setting

B.1. Benchmarks and Evaluation Metrics

CHAIR. CHAIR (Rohrbach et al., 2018) is a widely used benchmark for assessing object-level hallucinations in image captioning. It relies on ground-truth annotations of 80 object categories provided by the MSCOCO dataset (Lin et al., 2014) and measures hallucination from two complementary perspectives: $CHAIR_i = \frac{|\mathcal{O}_{hall}|}{|\mathcal{O}_{all}|}$, and $CHAIR_s = \frac{|\mathcal{C}_{hall}|}{|\mathcal{C}_{all}|}$. Here, \mathcal{O}_{hall} denotes the set of hallucinated object mentions that appear in the generated captions but are not present in the ground-truth annotations, and \mathcal{O}_{all} denotes the set of all object mentions in the generated captions. \mathcal{C}_{hall} denotes the set of generated captions that contain at least one hallucinated object, while \mathcal{C}_{all} denotes the set of all generated captions. Lower values of both $CHAIR_i$ and $CHAIR_s$ indicate fewer object hallucinations and better factual grounding in image descriptions. Following standard practice for evaluating LVLMs on CHAIR (Liu et al., 2024b; Xie et al., 2025; Zhao et al., 2025), we randomly sample 500 images from the COCO2014 validation set and prompt the models with “Please describe the image in detail”. Following Zhao et al. (2025), we additionally select another 500 samples for hyperparameter tuning.

SHR. SHR (Zhao et al., 2023b) is designed to evaluate hallucinations in fine-grained image descriptions. It is built on a subset of 200 images from the VG-100K dataset (Krishna et al., 2016), each of which is associated with detailed annotations including object categories, attributes, spatial relationships, and bounding boxes. To evaluate LVLMs, models are instructed to generate detailed image captions using the prompt “*Please describe this image in detail*”. The generated captions are subsequently assessed by a large language model (we use GPT-5-mini as a judge), which compares each sentence against the corresponding visual annotations and categorizes it as *Correct*, *Hallucination*, or *Cannot Judge* when the description is subjective or ambiguous. Based on these sentence-level judgments, SHR reports a set of fine-grained metrics and we use four representative ones, including *Hallucinated Sentences Per Image* (HSPI), *Hallucinated Words Per Image* (HWPI), *Hallucination Sentence Ratio* (HSR), and *Hallucination Word Ratio* (HWR). Lower values of these metrics indicate better factual alignment between generated captions and visual content.

POPE. POPE (Li et al., 2023) provides a discriminative evaluation protocol for object hallucinations in multimodal large language models. Instead of relying on free-form image captions, POPE reformulates hallucination assessment as a binary visual question answering task, where models are asked to answer simple yes-or-no questions about the existence of specific objects in an image (e.g., “*Is there a chair in the image?*”). This design enables a more controlled evaluation of object-level hallucinations. Model performance is reported using standard classification metrics, including Accuracy, Precision, Recall, and F1 score, offering a comprehensive view of both hallucination reduction and overall discriminative capability. Following Yin et al. (2025); Zhao et al. (2025), we report the averaged results across MSCOCO (Lin et al., 2014), A-QKVQA (Schwenk et al., 2022) and GQA (Hudson & Manning, 2019) on the POPE benchmark.

AMBER. AMBER (Wang et al., 2023) is a benchmark designed to assess hallucinations in LVLMs from both generative and discriminative perspectives. Compared to CHAIR, the AMBER dataset (Wang et al., 2023) covers a broader range of visual contexts, features more balanced object categories, and includes richer object-level annotations within each image. AMBER reports multiple evaluation metrics to characterize different aspects of hallucination behavior. Specifically, the *CHAIR* score in AMBER shares the same definition as *CHAIR_i*, while *Cover* measures object coverage and is analogous to recall. The *Hal* metric quantifies the proportion of generated responses that contain hallucinated content, and *Cog* reflects the degree to which model outputs are driven by language priors or commonsense reasoning rather than grounded visual evidence. Following the default AMBER evaluation protocol, we prompt the model with “*Describe this image.*”.

B.2. Baselines

For all the baseline methods we compare, we use default parameters they provided in the paper.

PAI. The attention boosting coefficient is set to $\alpha = 0.2$. The classifier-free guidance γ is set to 1.1 for LLaVA-NeXT, and 1.05 for Qwen3-VL and InternVL3.5, considering their higher visual token ratios. Attention boosting is applied to layers [0, 32) for LLaVA-NeXT and [4, 36) for Qwen3-VL and InternVL3.5, consistent with their respective model depths.

VAF. The visual enhancement parameter is set to $enh_para = 1.15$, and the system prompt suppression parameter is set to $sup_para = 0.90$. VAF is applied to the middle fusion layers [9, 15] across all models.

VGA. We set the attention coefficient to $\beta = 0.2$. We enable similarity-based head balancing and disable attention normalization, following the recommended configuration. The top- k parameter for entropy-based salience estimation is set to $k = 10$. Attention modulation is applied to layers [0, 15) for LLaVA-NeXT and [4, 15) for Qwen3-VL and InternVL3.5.

C. Additional Experiments

C.1. Full Experiment Results on AMBER

Table 4. Results on AMBER benchmark. The AMBER metric is calculated as $(1 - \text{CHAIR} + \text{F1})/2$.

MLLM	Method	CHAIR \downarrow	Cover \uparrow	Hal \downarrow	Cog \downarrow	Acc. \uparrow	Prec. \uparrow	Rec. \uparrow	F1 \uparrow	AMBER \uparrow
LLaVA-NeXT	Vanilla	7.83	63.87	49.20	4.33	85.28	90.42	87.03	88.69	90.43
	PAI	8.29	64.74	50.90	4.43	83.92	93.61	81.30	87.02	89.37
	VAF	7.64	63.24	47.41	3.70	84.24	90.64	85.00	87.72	90.04
	VGA	7.65	62.39	40.74	3.59	84.24	88.07	88.17	88.11	90.23
	Ours	6.97	61.21	39.85	3.41	85.08	90.20	86.92	88.52	90.78
Qwen3-VL	Vanilla	7.66	73.59	59.24	3.75	89.09	91.96	91.53	91.74	92.04
	PAI	8.23	74.11	63.39	3.50	88.93	91.72	91.56	91.63	91.70
	VAF	7.41	72.75	56.64	3.38	88.07	91.49	90.38	90.93	91.76
	VGA	7.97	73.32	60.31	3.34	88.60	92.17	90.47	91.31	91.67
	Ours	6.74	72.12	51.30	3.00	89.09	91.96	91.53	91.74	92.50
InternVL3.5	Vanilla	7.49	74.24	62.20	5.95	87.77	93.48	87.64	90.46	91.48
	PAI	8.51	74.88	66.00	5.29	87.68	93.82	87.13	90.35	90.92
	VAF	7.30	71.64	53.20	3.99	87.17	93.89	86.23	89.89	91.30
	VGA	7.36	73.99	62.09	5.49	88.06	93.99	87.57	90.66	91.65
	Ours	6.50	72.30	50.24	2.78	87.77	93.48	87.64	90.46	91.98

C.2. Full Experiment Results on POPE

Table 5. Results on POPE. The results reported as the average performance across the MSCOCO, A-OKVQA, and GQA datasets.

Method	LLaVA-NeXT				Qwen3-VL				InternVL3.5			
	Acc. \uparrow	Prec. \uparrow	Rec. \uparrow	F1 \uparrow	Acc. \uparrow	Prec. \uparrow	Rec. \uparrow	F1 \uparrow	Acc. \uparrow	Prec. \uparrow	Rec. \uparrow	F1 \uparrow
Random												
Vanilla	91.34	89.71	93.80	91.57	93.24	95.04	91.37	93.09	90.96	89.66	92.64	91.08
PAI	90.36	87.27	95.13	90.85	93.23	93.89	92.62	93.17	90.17	87.66	93.62	90.51
VAF	90.24	86.46	95.89	90.80	93.10	93.14	93.22	93.09	91.70	89.08	95.17	91.99
VGA	90.83	89.31	93.29	91.08	92.82	94.30	91.29	92.68	92.32	90.58	94.53	92.48
Ours	91.33	89.70	93.78	91.55	93.16	95.18	91.06	92.99	91.26	88.52	94.97	91.59
Popular												
Vanilla	86.01	81.83	93.82	87.15	88.48	86.61	91.35	88.80	82.85	77.60	92.59	84.35
PAI	84.09	78.83	95.13	85.88	88.45	85.78	92.60	88.92	81.28	75.18	93.53	83.31
VAF	84.64	78.86	95.89	86.33	87.14	83.45	93.11	87.88	82.84	76.45	95.17	84.74
VGA	83.45	78.94	93.22	85.12	87.46	84.97	91.29	87.90	83.31	77.31	94.50	85.00
Ours	86.01	81.85	93.80	87.14	88.35	86.61	91.04	88.64	82.64	76.32	94.91	84.55
Adversarial												
Vanilla	80.18	74.47	93.82	82.72	84.11	80.25	91.35	85.24	78.68	72.71	92.59	81.30
PAI	77.23	70.95	95.13	80.93	83.55	78.96	92.60	85.00	77.22	70.71	93.53	80.44
VAF	77.81	71.01	95.89	81.36	82.39	77.17	93.11	84.17	78.48	71.55	95.17	81.61
VGA	77.46	71.87	93.22	80.77	83.05	78.85	91.29	84.40	78.71	72.04	94.50	81.66
Ours	80.15	74.46	93.80	82.70	84.09	80.38	91.04	85.17	78.46	71.61	94.91	81.54

C.3. Ablation Study

Table 6. Ablation study on method components (CHAIR benchmark).

Method	LLaVA-NeXT			Qwen3-VL			InternVL3.5		
	CHAIRs↓	CHAIRi↓	F1↑	CHAIRs↓	CHAIRi↓	F1↑	CHAIRs↓	CHAIRi↓	F1↑
Vanilla	33.80	8.46	71.44	58.80	10.57	75.29	41.40	10.80	74.71
+ Text Suppression	31.60	8.00	71.24	52.40	9.98	74.39	39.20	10.45	74.70
+ Visual Boosting	28.80	7.66	71.18	46.00	8.38	75.22	34.40	9.34	75.32

Table 7. Ablation study on text suppression scope (CHAIR benchmark).

Suppression Scope	LLaVA-NeXT			Qwen3-VL			InternVL3.5		
	CHAIRs↓	CHAIRi↓	F1↑	CHAIRs↓	CHAIRi↓	F1↑	CHAIRs↓	CHAIRi↓	F1↑
All Text Tokens	26.40	7.89	69.63	41.80	7.79	74.18	38.40	10.49	75.08
Text Output Only	33.20	9.05	71.49	55.20	10.97	74.46	38.80	10.75	74.44
System Prompt Only	31.80	9.60	70.69	50.00	8.93	74.63	33.60	9.95	74.74
Text Input Only	28.80	7.66	71.18	46.00	8.38	75.22	34.40	9.34	75.32

C.4. Sensitivity Analysis

C.4.1. BALANCE COEFFICIENT α

 Table 8. Sensitivity analysis on balance coefficient α (CHAIR benchmark).

α	LLaVA-NeXT			Qwen3-VL			InternVL3.5		
	CHAIRs↓	CHAIRi↓	F1↑	CHAIRs↓	CHAIRi↓	F1↑	CHAIRs↓	CHAIRi↓	F1↑
0.5	28.80	7.66	71.18	46.00	8.58	75.44	35.80	9.66	74.31
0.6	29.00	7.52	71.06	46.00	8.38	75.22	35.40	9.87	74.94
0.7	28.60	7.59	70.95	48.80	8.80	75.38	34.80	9.46	75.12
0.8	29.40	7.96	70.85	49.40	9.25	75.92	34.40	9.34	75.32
0.9	30.40	7.98	71.18	46.60	9.39	75.69	35.60	9.78	75.02
1.0	29.80	8.03	71.69	50.20	9.31	74.66	34.20	9.26	75.08

C.4.2. RISK SCALE γ

 Table 9. Sensitivity analysis on risk scale γ (CHAIR benchmark).

γ	LLaVA-NeXT			Qwen3-VL			InternVL3.5		
	CHAIRs↓	CHAIRi↓	F1↑	CHAIRs↓	CHAIRi↓	F1↑	CHAIRs↓	CHAIRi↓	F1↑
0.5	28.80	7.66	71.18	43.60	8.19	75.08	35.20	9.97	74.68
0.6	29.00	7.85	70.97	46.00	8.38	75.22	34.80	10.24	75.46
0.7	29.00	7.53	71.13	48.20	8.81	75.50	34.40	9.34	75.32
0.8	29.60	7.69	70.75	47.80	9.21	75.40	32.60	8.88	75.08
0.9	30.60	8.06	70.36	51.20	8.57	75.40	34.00	9.86	75.03
1.0	29.60	7.91	71.10	50.00	10.79	74.59	34.60	9.25	74.83

C.4.3. MAXIMUM VISUAL BOOSTING FACTOR m_{vis}^{\max}

 Table 10. Sensitivity analysis on maximum visual boosting factor m_{vis}^{\max} (CHAIR benchmark).

m_{vis}^{\max}	LLaVA-NeXT			Qwen3-VL			InternVL3.5		
	CHAIRs \downarrow	CHAIRi \downarrow	F1 \uparrow	CHAIRs \downarrow	CHAIRi \downarrow	F1 \uparrow	CHAIRs \downarrow	CHAIRi \downarrow	F1 \uparrow
1.1	28.80	7.66	71.18	48.80	8.31	75.40	35.40	9.40	75.06
1.2	29.00	7.75	71.05	51.20	8.56	75.40	33.40	9.08	75.49
1.3	30.60	7.47	70.66	46.00	8.38	75.22	34.40	9.34	75.32
1.4	30.60	7.43	70.67	39.60	7.97	74.98	34.60	9.58	75.54
1.5	31.60	7.61	70.94	33.60	7.39	71.92	35.40	10.22	75.03
1.6	31.40	7.49	70.83	25.20	4.57	68.71	33.20	9.36	74.90
1.7	31.40	8.52	70.22	21.00	4.49	65.56	35.20	9.63	75.32
1.8	31.00	8.60	70.86	15.80	3.73	62.48	35.40	9.59	74.52
1.9	30.20	8.00	70.54	13.80	4.01	58.88	33.60	9.74	75.38
2.0	30.20	8.33	70.16	7.40	2.74	55.88	35.20	10.58	74.61

 C.4.4. MAXIMUM TEXTUAL SUPPRESSION FACTOR m_{txt}^{\max}

 Table 11. Sensitivity analysis on maximum textual suppression factor m_{txt}^{\max} (CHAIR benchmark).

m_{txt}^{\max}	LLaVA-NeXT			Qwen3-VL			InternVL3.5		
	CHAIRs \downarrow	CHAIRi \downarrow	F1 \uparrow	CHAIRs \downarrow	CHAIRi \downarrow	F1 \uparrow	CHAIRs \downarrow	CHAIRi \downarrow	F1 \uparrow
1.1	35.40	8.69	72.40	53.80	10.48	74.81	41.20	11.08	74.28
1.2	35.60	9.09	71.08	53.60	10.15	75.00	39.20	10.79	74.65
1.3	33.40	8.52	71.14	46.00	8.38	75.22	40.00	10.49	75.00
1.4	33.00	8.92	71.35	41.20	8.37	74.36	38.80	10.14	75.03
1.5	33.00	8.77	70.55	42.20	7.89	73.54	35.80	9.63	74.64
1.6	30.00	8.09	71.53	41.80	8.55	72.84	34.40	9.34	75.32
1.7	28.80	7.66	71.18	36.80	7.78	72.88	33.60	9.54	74.81
1.8	28.00	7.15	71.00	36.80	8.31	71.41	29.80	9.06	74.09
1.9	28.60	7.33	70.27	35.80	7.76	72.39	33.20	9.40	74.76
2.0	33.20	9.49	70.53	35.60	7.05	73.63	32.60	9.39	73.59